

# Acoustic scaling of linear and mode-coupled anisotropic flow; implications for precision extraction of the specific shear viscosity

Peifeng Liu<sup>1,2</sup> and Roy A. Lacey<sup>1,2,\*</sup>

<sup>1</sup>*Department of Chemistry, Stony Brook University,  
Stony Brook, NY, 11794-3400, USA*

<sup>2</sup>*Department of Physics and Astronomy, Stony Brook University,  
Stony Brook, NY, 11794-3800*

(Dated: January 27, 2019)

The scaling properties of the  $n^{\text{th}}$ -order linear flow coefficients  $v_n^L$  ( $n = 2, 3, 4, 5$ ), and the corresponding nonlinear mode-coupled (mc) coefficients  $v_{4,(2,2)}^{\text{mc}}$ ,  $v_{5,(2,3)}^{\text{mc}}$ ,  $v_{6,(3,3)}^{\text{mc}}$  and  $v_{6,(2,2,2)}^{\text{mc}}$ , are studied for Pb+Pb collisions at  $\sqrt{s_{\text{NN}}} = 2.76$  TeV. Both sets of coefficients indicate a common acoustic scaling pattern of exponential viscous modulation, at a rate proportional to the square of the harmonic numbers and the mean transverse momenta (respectively), and inversely proportional to the cube root of the charge particle multiplicity ( $(N_{\text{ch}})^{1/3}$ ), that characterizes the dimensionless size of the systems produced in the collisions. These patterns and their associated scaling parameters, provide new stringent constraints for eccentricity independent estimates of the specific shear viscosity ( $\eta/s$ ) of the matter produced in the collisions, as well as simultaneous extraction of the initial-state eccentricity spectrum.

PACS numbers:

Anisotropic flow measurements play a crucial role in ongoing studies of the properties of the high energy-density quark-gluon plasma (QGP) created in relativistic heavy-ion collisions [1–8]. In particular, they provide an important avenue for the extraction of the specific shear viscosity (i.e., the ratio of shear viscosity to entropy density  $\eta/s$ ) of the QGP, since they encode the viscous hydrodynamic response to the anisotropic transverse energy density profile produced in the early stages of the collision [3, 5–10].

In experiments, this flow manifests as an azimuthal asymmetry of the measured single-particle distribution and is routinely quantified by the complex flow vectors [9–11]:

$$V_n \equiv v_n e^{in\Psi_n} \equiv \{e^{in\phi}\}, \quad v_n = \left\langle |V_n|^2 \right\rangle^{1/2}, \quad (1)$$

where  $\phi$  denotes the azimuthal angle around the beam direction, of a particle emitted in the collision,  $\{\dots\}$  denotes the average over all particles emitted in the event, and  $v_n$  and  $\Psi_n$  denote the magnitude and azimuthal direction of the  $n^{\text{th}}$ -order harmonic flow vector which fluctuates from event to event. The coefficients  $v_2$  and  $v_3$  are commonly termed elliptic- and triangular flow respectively.

The initial anisotropic density profile  $\rho_e(r, \varphi)$  (in the transverse plane) which drives anisotropic flow, can be similarly characterized by complex eccentricity coefficients [12–16]:

$$\mathcal{E}_n \equiv \varepsilon_n e^{in\Phi_n} \equiv - \frac{\int d^2r_{\perp} r^m e^{in\varphi} \rho_e(r, \varphi)}{\int d^2r_{\perp} r^m \rho_e(r, \varphi)}, \quad (2)$$

where  $\varepsilon_n = \left\langle |\mathcal{E}_n|^2 \right\rangle^{1/2}$  and  $\Phi_n$  denote the magnitude and azimuthal direction of the  $n^{\text{th}}$ -order eccentricity vector

which also fluctuates from event to event;  $m = n$  for  $n \geq 2$  and  $m = 3$  for  $n = 1$  [15].

Theoretical investigations show that  $v_n \propto \varepsilon_n$  for elliptic- and triangular flow ( $n = 2$  and  $3$ ) [16–19], albeit with a small anti-correlation between  $v_2$  and  $v_3$  [20, 21], which derives from an anti-correlation between  $\varepsilon_2$  and  $\varepsilon_3$  [22]; the latter is more important for peripheral collisions. Because the specific shear viscosity  $\eta/s$ , reduces the values of  $v_n$  and hence, the ratio  $v_n/\varepsilon_n$ , viscous hydrodynamical model comparisons to this ratio (implicit and explicit) have been employed to estimate  $\eta/s$  [3, 5, 7, 8, 16, 23–26]. Such estimates have indicated a small value (i.e. 1-3 times the lower conjectured bound of  $1/4\pi$  [27]), with substantial uncertainties of  $\mathcal{O}(100\%)$ , primarily due to the lack of constraints for  $\varepsilon_n$  and its fluctuations. Thus, there is a pressing need to develop new experimental constraints that can reduce this critical bottleneck for precision extraction of  $\eta/s$ .

The higher order flow coefficients for  $n > 3$ , reflect a linear response related to  $\varepsilon_n$ , as well as nonlinear mode-couplings derived from lower-order harmonics driven by eccentricities of the same harmonic order [10, 28, 29]:

$$V_4 = V_4^L + \chi_{4,(2,2)}^{\text{mc}} (V_2)^2, \quad (3)$$

$$V_5 = V_5^L + \chi_{5,(2,3)}^{\text{mc}} V_2 V_3, \quad (4)$$

$$V_6 = V_6^L + \chi_{6,(2,2,2)}^{\text{mc}} (V_2)^3 + \chi_{6,(3,3)}^{\text{mc}} (V_3)^2, \quad (5)$$

$$V_7 = V_7^L + \chi_{7,(2,2,3)}^{\text{mc}} (V_2)^2 V_3, \quad (6)$$

where  $\chi_{n,(i,j)}^{\text{mc}}$  and  $\chi_{n,(i,i,j)}^{\text{mc}}$  ( $i = 2, j = 2, 3$ ) are  $n^{\text{th}}$ -order nonlinear mode-coupling coefficients. In Eqs. 5 and 6 the nonlinear contributions are restricted to the two largest flow coefficients,  $V_2$  and  $V_3$  [10, 29].

If the linear and non-linear terms in Eqs. 3 - 6 are uncorrelated, the mode-coupling coefficients can be ex-

pressed as [10, 29]:

$$\begin{aligned}\chi_{4,(2,2)}^{\text{mc}} &= \frac{\text{Re}\langle V_4(V_2^*)^2 \rangle}{\langle v_2^4 \rangle}, & \chi_{5,(2,3)}^{\text{mc}} &= \frac{\text{Re}\langle V_5 V_2^* V_3^* \rangle}{\langle v_2^2 v_3^2 \rangle}, \\ \chi_{6,(3,3)}^{\text{mc}} &= \frac{\text{Re}\langle V_6(V_3^*)^2 \rangle}{\langle v_3^4 \rangle}, & \chi_{6,(2,2,2)}^{\text{mc}} &= \frac{\text{Re}\langle V_6(V_2^*)^3 \rangle}{\langle v_2^6 \rangle}, \\ \chi_{7,(2,2,3)}^{\text{mc}} &= \frac{\text{Re}\langle V_7(V_2^*)^2 V_3^* \rangle}{\langle v_2^4 v_3^2 \rangle}.\end{aligned}\quad (7)$$

The magnitudes of the mode-coupled flow vectors can also be expressed in terms of the correlations of  $V_n$  with  $\Psi_2$  and  $\Psi_3$  to give [29, 30]:

$$\begin{aligned}v_{4,(2,2)}^{\text{mc}} &= \frac{\langle v_4 v_2^2 \cos(4\Psi_4 - 4\Psi_2) \rangle}{\sqrt{\langle v_2^4 \rangle}} \approx \langle v_4 \cos(4\Psi_4 - 4\Psi_2) \rangle, \\ v_{5,(3,2)}^{\text{mc}} &= \frac{\langle v_5 v_3 v_2 \cos(5\Psi_5 - 3\Psi_3 - 2\Psi_2) \rangle}{\sqrt{\langle v_3^2 v_2^2 \rangle}} \\ &\approx \langle v_5 \cos(5\Psi_5 - 3\Psi_3 - 2\Psi_2) \rangle, \\ v_{6,(2,2,2)}^{\text{mc}} &= \frac{\langle v_6 v_2^3 \cos(6\Psi_6 - 6\Psi_2) \rangle}{\sqrt{\langle v_2^6 \rangle}} \approx \langle v_6 \cos(6\Psi_6 - 6\Psi_2) \rangle, \\ v_{6,(3,3)}^{\text{mc}} &= \frac{\langle v_6 v_3^2 \cos(6\Psi_6 - 6\Psi_3) \rangle}{\sqrt{\langle v_3^4 \rangle}} \approx \langle v_6 \cos(6\Psi_6 - 6\Psi_3) \rangle,\end{aligned}$$

which points to the important role of event-plane correlations for mode-coupling. It is also straight forward to use Eqs. 3 - 7 to evaluate the magnitude of the higher-order linear harmonic response:

$$v_4^{\text{L}} = \sqrt{v_4^2 - v_{4,(2,2)}^2}, \quad v_5^{\text{L}} = \sqrt{v_5^2 - v_{5,(3,2)}^2}. \quad (8)$$

Analogous to anisotropic flow, the complex eccentricity coefficients defined in Eq. 2, can be used to determine the higher-order mixed-mode eccentricities:

$$\begin{aligned}\varepsilon_n &= \sqrt{\langle |\mathcal{E}_n|^2 \rangle}, & \varepsilon_{4,(2,2)}^{\text{mc}} &= \sqrt{\langle \varepsilon_4^2 \rangle}, \\ \varepsilon_{5,(2,3)}^{\text{mc}} &= \sqrt{\langle \varepsilon_2^2 \varepsilon_3^2 \rangle}, & \varepsilon_{6,(3,3)}^{\text{mc}} &= \sqrt{\langle \varepsilon_3^4 \rangle}, \\ \varepsilon_{6,(2,2,2)}^{\text{mc}} &= \sqrt{\langle \varepsilon_2^6 \rangle}, & \varepsilon_{7,(2,2,3)}^{\text{mc}} &= \sqrt{\langle \varepsilon_2^4 \varepsilon_3^2 \rangle}.\end{aligned}\quad (9)$$

Recently, it has been argued that the linear response contribution to higher-order flow, should be linearly proportional to the cumulant-defined eccentricities  $\mathcal{E}'_n$  instead of  $\mathcal{E}_n$  [10]:

$$\begin{aligned}\mathcal{E}'_2 &\equiv \varepsilon_2 e^{i2\Phi_2} = \mathcal{E}_2, & \mathcal{E}'_3 &\equiv \varepsilon_3 e^{i3\Phi_3} = \mathcal{E}_3, \\ \mathcal{E}'_4 &\equiv \varepsilon'_4 e^{i4\Phi'_4} \equiv -\frac{\langle z^4 \rangle - 3\langle z^2 \rangle^2}{\langle r^4 \rangle} = \mathcal{E}_4 + \frac{3\langle r^2 \rangle^2}{\langle r^4 \rangle} \mathcal{E}_2^2, \\ \mathcal{E}'_5 &\equiv \varepsilon'_5 e^{i5\Phi'_5} \equiv -\frac{\langle z^5 \rangle - 10\langle z^2 \rangle \langle z^3 \rangle}{\langle r^5 \rangle} = \mathcal{E}_5 + \frac{10\langle r^2 \rangle \langle r^3 \rangle}{\langle r^5 \rangle} \mathcal{E}_2 \mathcal{E}_3,\end{aligned}\quad (10)$$

where  $z \equiv x + iy = r e^{i\phi}$ . An important advantage of this definition, is that it allows the subtraction of contributions from lower order  $z$  correlations.

The specific shear viscosity attenuates  $v_n^{\text{L}}/\varepsilon'_n$ ,  $v_{n,(i,j)}^{\text{mc}}/\varepsilon_{n,(i,j)}^{\text{mc}}$  and  $v_{n,(i,i,j)}^{\text{mc}}/\varepsilon_{n,(i,i,j)}^{\text{mc}}$ . For measurements at a given mean transverse momentum  $\langle p_T \rangle$ , and centrality cent, this viscous damping can be expressed via an acoustic ansatz [22, 31–33] as:

$$\frac{v_n^{\text{L}}}{\varepsilon_n} \propto \exp\left(-n^2 \beta \frac{1}{\text{RT}}\right), \quad (11)$$

$$\frac{v_{n,(i,j)}^{\text{mc}}}{\varepsilon_{n,(i,j)}^{\text{mc}}} \propto \exp\left(-(i^2 + j^2) \beta \frac{1}{\text{RT}}\right),$$

$$\frac{v_{n,(i,i,j)}^{\text{mc}}}{\varepsilon_{n,(i,i,j)}^{\text{mc}}} \propto \exp\left(-2i^2 + j^2 \beta \frac{1}{\text{RT}}\right), \quad (12)$$

where  $\beta \propto \eta/s$ ,  $T$  is the temperature and  $R$  characterizes the geometric size of the collision zone. For a given centrality selection, the dimensionless size  $\text{RT} \propto N_{\text{ch}}^{1/3}$  where  $N_{\text{ch}}$  is the charged particle multiplicity density in one unit of pseudorapidity [34].

Equations 11 and 12 suggest characteristic linear dependencies for  $\ln(v_n^{\text{L}}/\varepsilon'_n)$ ,  $\ln(v_{n,(i,j)}^{\text{mc}}/\varepsilon_{n,(i,j)}^{\text{mc}})$  and  $\ln(v_{n,(i,i,j)}^{\text{mc}}/\varepsilon_{n,(i,i,j)}^{\text{mc}})$  on  $\langle N_{\text{ch}} \rangle^{-1/3}$  (respectively), with slopes that reflect specific quadratic viscous attenuation prefactors for  $\beta$ ; these combined features are termed acoustic scaling. Thus, the prefactors, reflected in the slopes of  $\ln(v_n^{\text{L}}/\varepsilon'_n)$  vs.  $\langle N_{\text{ch}} \rangle^{-1/3}$  are not only expected to increase as  $n^2$ , but should be approximately 2-3 times larger than those for  $v_{n,(i,j)}^{\text{mc}}/\varepsilon_{n,(i,j)}^{\text{mc}}$  and  $v_{n,(i,i,j)}^{\text{mc}}/\varepsilon_{n,(i,i,j)}^{\text{mc}}$  vs.  $\langle N_{\text{ch}} \rangle^{-1/3}$  (respectively) since  $(i^2 + j^2) < n^2$ .

Independent estimates of  $\beta$ , involving very different eccentricities, can also be obtained from the linear and mode-coupled harmonics. For example, the slope of the double ratio  $[(v_{5,(2,3)}^{\text{mc}}/\varepsilon_{5,(2,3)}^{\text{mc}})/(v_2^{\text{L}}/\varepsilon_2)]$  vs.  $\langle N_{\text{ch}} \rangle^{-1/3}$ , is expected to be the same as that for  $\ln(v_3^{\text{L}}/\varepsilon_3)$  vs.  $\langle N_{\text{ch}} \rangle^{-1/3}$ . Thus, the validation of simultaneous acoustic scaling of the linear and mode-coupled harmonics to give a single estimate of  $\beta \propto \eta/s$ , could provide a powerful constraint for initial-state eccentricity models and precision extraction of  $\eta/s$ .

In this letter, we use recent measurements of the linear and mode-coupled harmonics in Pb+Pb collisions at  $\sqrt{s_{NN}} = 2.76$  TeV, to explore validation tests for simultaneous acoustic scaling of  $v_n^{\text{L}}/\varepsilon'_n$ ,  $v_{n,(i,j)}^{\text{mc}}/\varepsilon_{n,(i,j)}^{\text{mc}}$  and  $v_{n,(i,i,j)}^{\text{mc}}/\varepsilon_{n,(i,i,j)}^{\text{mc}}$ , with an eye towards the development of new experimental constraints which could significantly reduce the large eccentricity-driven uncertainties associated with current extractions of  $\eta/s$ .

The data employed in this work are taken from the published flow measurements for Pb+Pb collisions at  $\sqrt{s_{NN}} = 2.76$  TeV by the ALICE [35, 36] and ATLAS [20] collaborations. The ALICE centrality dependent  $p_T$ -integrated measurements were performed for the harmonics  $n = 2, 3, 4, 5, 6$ , for charged particles with pseudorapidity difference  $|\Delta\eta| < 0.8$  and  $0.2 < p_T < 5.0$  GeV/c. Both the linear and mode-coupled flow coefficients were

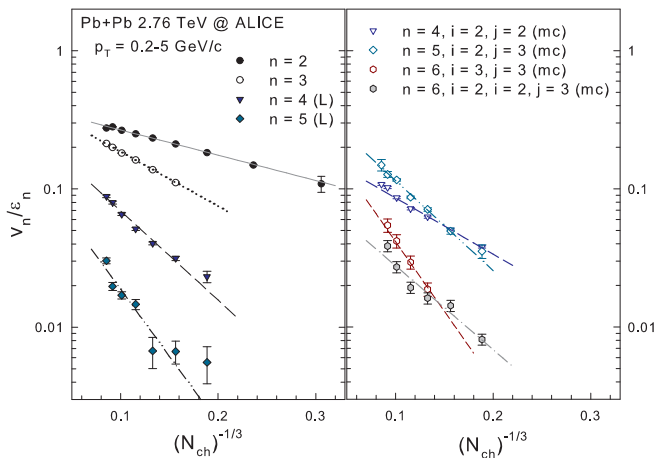


FIG. 1. Comparison of  $\ln(v_n^L/\epsilon_n)$  vs.  $(N_{\text{ch}})^{-1/3}$  for the linear harmonics (left panel), and  $v_{n,(i,j)}^{\text{mc}}/\epsilon_{n,(i,j)}^{\text{mc}}$  vs.  $(N_{\text{ch}})^{-1/3}$  (respectively) for the nonlinear mode-coupled harmonics, for Pb+Pb collisions at at  $\sqrt{s_{NN}} = 2.76$  TeV. The lines represent a simultaneous exponential fit to the data, following Eqs. 11 and 12. The ALICE data are taken from Refs. [35, 36].

obtained directly via a two sub-events multiparticle correlation method. The corresponding ATLAS measurements were performed for  $n = 2, 3, 4, 5$  for particles with  $2 < |\Delta\eta| < 5$  and for several  $p_T$  selections spanning the range  $0.5 < p_T < 4.0$  GeV/c, with the two-particle correlation method supplemented with event-shape selection [20]. The systematic uncertainties, which are included in our scaling analyses, are reported in Refs. [20, 35, 36] for both sets of measurements.

The requisite cumulant-defined eccentricities were calculated following the procedure outlined in Eqs. 2, 9 and 10 with the aid of a Monte Carlo quark-Glauber model (MC-qGlauber) with fluctuating initial conditions [37]. The model, which is based on the commonly used MC-Glauber model [38], was used to compute the number of quark participants  $N_{\text{qpart}}(\text{cent})$ ,  $\epsilon'_n(\text{cent})$  and  $\epsilon_n^{\text{mc}}(\text{cent})$  from the two-dimensional profile of the density of sources in the transverse plane  $\rho_s(\mathbf{r}_\perp)$  [10, 14, 37]. The model takes account of the finite size of the nucleon, the wounding profile of the nucleon, the distribution of quarks inside the nucleon and quark cross sections which reproduce the NN inelastic cross section at  $\sqrt{s_{NN}} = 2.76$  TeV. A systematic uncertainty of 2-5% was estimated for the eccentricities from variations of the model parameters.

The centrality dependent multiplicity densities used to evaluate the dimensionless size  $RT \propto N_{\text{ch}}^{1/3}$ , are obtained from ALICE [39] and ATLAS [40] multiplicity density measurements. Validation tests for acoustic scaling were performed by plotting  $v_n^L/\epsilon_n$ ,  $v_{n,(i,j)}^{\text{mc}}/\epsilon_{n,(i,j)}^{\text{mc}}$  and  $v_{n,(i,i,j)}^{\text{mc}}/\epsilon_{n,(i,i,j)}^{\text{mc}}$  vs.  $(N_{\text{ch}})^{-1/3}$  respectively, to test for the expected patterns and the relative viscous attenuation  $\beta$ -prefactors indicated in Eqs. 11 and 12.

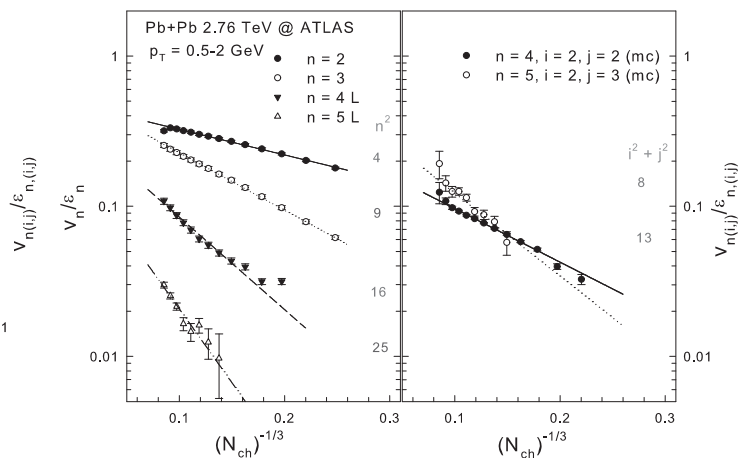


FIG. 2. Same as Fig. 1 but for ATLAS data [20]; the  $\beta$ -prefactors  $n^2$  and  $(i^2 + j^2)$  are indicated in the figure.

Figures 1 and 2 show the plots for  $v_n^L/\epsilon_n$ ,  $v_{n,(i,j)}^{\text{mc}}/\epsilon_{n,(i,j)}^{\text{mc}}$  and  $v_{n,(i,i,j)}^{\text{mc}}/\epsilon_{n,(i,i,j)}^{\text{mc}}$  vs.  $(N_{\text{ch}})^{-1/3}$  (respectively), for the ALICE (Fig. 1) and ATLAS (Fig. 2) data sets. They indicate the telltale acoustic scaling patterns of a characteristic linear dependence of  $\ln(v_n^L/\epsilon_n)$ ,  $\ln(v_{n,(i,j)}^{\text{mc}}/\epsilon_{n,(i,j)}^{\text{mc}})$  and  $\ln(v_{n,(i,i,j)}^{\text{mc}}/\epsilon_{n,(i,i,j)}^{\text{mc}})$  on  $(N_{\text{ch}})^{-1/3}$  (respectively), with slope factors which strongly depend on the harmonic number  $n$  and the values of the mode-coupled harmonics  $i, j$  and  $i, i, j$ . Note that the slopes for the linear harmonics (left panel in each figure) show a much steeper dependence on  $(N_{\text{ch}})^{-1/3}$  than those for the mode-coupled harmonics (right panel in each figure), as expected from Eqs. 11 and 12. The expected slope hierarchy for both the linear and mode-coupled results are also apparent in both figures. The qualitative similarities between the results shown in Figs. 1 and 2 suggest that the respective methods employed by ATLAS and ALICE for extraction of the flow coefficients, are complementary.

The lines shown in Figs. 1 and 2 represent the results from fits to the data following Eqs. 11 and 12. They indicate that, within an uncertainty of  $\sim 5 - 10\%$ , a single slope value  $\beta$ , can account for the wealth of the linear and mode-coupled measurements in each data set. That is, they confirm the quadratic  $\beta$  pre-factors of 4, 9, 16 and 25 for  $v_n^L$  ( $n=2,3,4$  and 5) and 8, 13, 18 and 12 for  $v_{4,(2,2)}^{\text{mc}}$ ,  $v_{5,(2,3)}^{\text{mc}}$ ,  $v_{6,(3,3)}^{\text{mc}}$  and  $v_{6,(2,2,2)}^{\text{mc}}$  respectively. To estimate the fit uncertainty for each data set, the slope for the fit to  $v_2/\epsilon_2$  was first obtained, and then used in conjunction with the quadratic pre-factors divided by 4, to quantify slope deviations from one.

The  $p_T$  dependence of the viscous attenuation of the flow coefficients can also be used to constrain the magnitude of the first viscous correction  $\delta f$ , to the thermal distribution function [41], employed in viscous hydrodynamical model calculations. This correction factor is  $\propto p_T^k$ , where current theoretical estimates indicate the

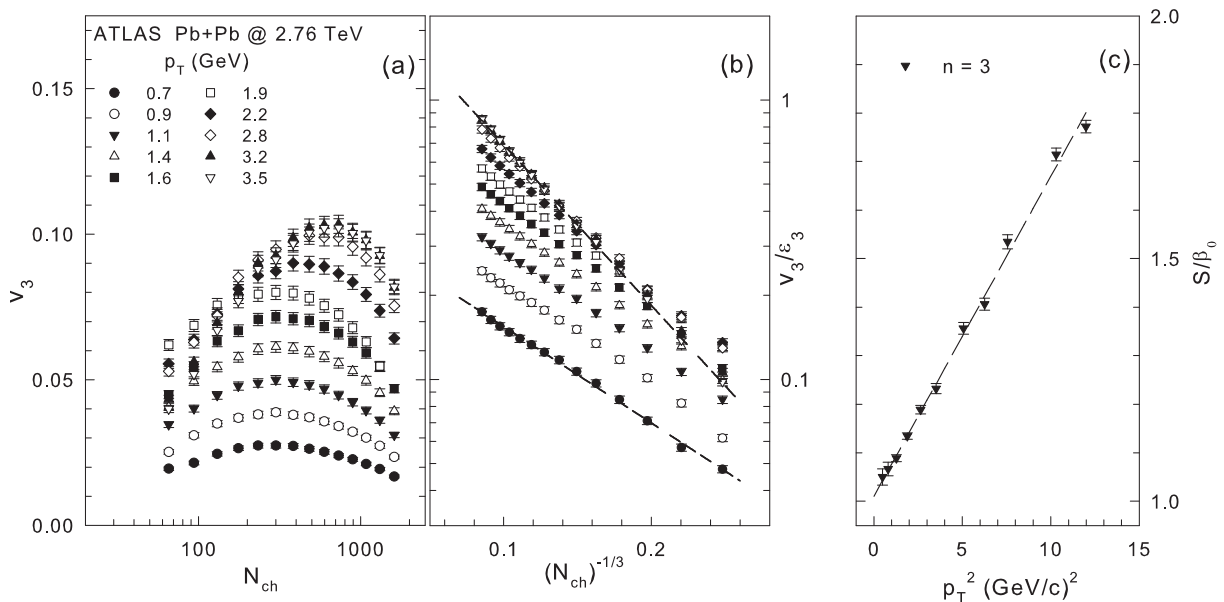


FIG. 3. (a)  $v_3$  vs.  $N_{ch}$  for several  $\langle p_T \rangle$  selections as indicated; (b)  $v_3/\varepsilon_3$  vs.  $(N_{ch})^{-1/3}$  for the data shown in (a). The dashed lines represent an exponential fit to the data for the selections  $\langle p_T \rangle = 0.7$  and  $3.5$  GeV/c respectively. (c)  $S/\beta_0$  vs.  $\langle p_T \rangle^2$ ; the slopes  $S$ , are obtained from fits to the eccentricity-scaled data in (b). The ATLAS data used in the plots are taken from Ref. [20]

range 1-2 for  $k$  [41]. The influence of this viscous correction can be seen in Fig. 3(a), which shows that the viscous suppression of  $v_3$  increases with  $p_T$ , especially for the lower values of  $N_{ch}$ ; note the rather steep fall-off of  $v_3$  with  $p_T$ , for  $N_{ch} \lesssim 400$ . This suppression is made more transparent in Fig. 3(b), where the characteristic linear dependence of  $\ln(v_3/\varepsilon_3)$  on  $(N_{ch})^{-1/3}$ , with slopes ( $S$ ) which strongly depend on  $p_T$ , can be observed for  $p_T$ -selections spanning the range  $0.7 \leq p_T \leq 3.5$  GeV/c. Fig. 3(c) shows that the slopes increase as  $p_T^2$  for the indicated range, and can grow to a value  $\sim 1.8\beta_0$ , where  $\beta_0$  is the slope extrapolated to  $p_T = 0.0$  GeV/c.

The present analysis shows that an eccentricity independent estimate of  $\beta \propto \eta/s$  is very well constrained by simultaneous acoustic scaling of both the linear and mode-coupled flow coefficients. However, a further calibration would be required to map  $\beta(\beta_0)$  on to the the actual value of  $\eta/s$  for the QGP. An appropriately constrained set of viscous hydrodynamical calculations, tuned to reproduce the results shown in Figs. 1 - 3, could provide such a calibration to give a relatively precise estimate of  $\eta/s$ , as well as simultaneous verification of the initial-state eccentricity spectrum.

In summary, we have presented a detailed phenomenological investigation for new constraints designed to facilitate precision extraction of  $\eta/s$ . We find that the linear flow coefficients  $v_n^L$  ( $n = 2, 3, 4, 5$ ), and the nonlinear mode-coupled coefficients  $v_{4,(2,2)}^{mc}$ ,  $v_{5,(2,3)}^{mc}$ ,  $v_{6,(3,3)}^{mc}$  and  $v_{6,(2,2,2)}^{mc}$ , follow a common acoustic scaling pattern of exponential viscous modulation in the created medium, at

a rate proportional to the square of the harmonic numbers and the transverse momenta (respectively), and inversely proportional to  $(N_{ch})^{1/3}$  which serves as a proxy for the dimensionless size of the systems produced in the collisions. These patterns and their associated scaling parameters, could provide stringent new constraints for eccentricity independent estimates of  $\eta/s$ , and the initial-state eccentricity spectrum.

**Acknowledgments** This research is supported by the US DOE under contract DE-FG02-87ER40331.A008.

\* E-mail: Roy.Lacey@Stonybrook.edu

- [1] D. Teaney, Phys.Rev. **C68**, 034913 (2003), arXiv:nucl-th/0301099 [nucl-th].
- [2] R. A. Lacey and A. Taranenko, PoS **CFRNC2006**, 021 (2006), arXiv:nucl-ex/0610029 [nucl-ex].
- [3] P. Romatschke and U. Romatschke, Phys.Rev.Lett. **99**, 172301 (2007), arXiv:0706.1522 [nucl-th].
- [4] M. Luzum and P. Romatschke, Phys.Rev. **C78**, 034915 (2008), arXiv:0804.4015 [nucl-th].
- [5] H. Song, S. A. Bass, U. Heinz, T. Hirano, and C. Shen, Phys. Rev. Lett. **106**, 192301 (2011), [Erratum: Phys. Rev. Lett.109,139904(2012)], arXiv:1011.2783 [nucl-th].
- [6] J. Qian, U. W. Heinz, and J. Liu, Phys. Rev. **C93**, 064901 (2016), arXiv:1602.02813 [nucl-th].
- [7] B. Schenke, S. Jeon, and C. Gale, Phys.Lett. **B702**, 59 (2011), arXiv:1102.0575 [hep-ph].

- [8] F. G. Gardim, F. Grassi, M. Luzum, and J.-Y. Ollitrault, *Phys.Rev.Lett.* **109**, 202302 (2012), arXiv:1203.2882 [nucl-th].
- [9] M. Luzum, *J. Phys.* **G38**, 124026 (2011), arXiv:1107.0592 [nucl-th].
- [10] D. Teaney and L. Yan, *Phys. Rev.* **C86**, 044908 (2012), arXiv:1206.1905 [nucl-th].
- [11] J.-Y. Ollitrault, *Phys. Rev.* **D46**, 229 (1992).
- [12] B. H. Alver, C. Gombeaud, M. Luzum, and J.-Y. Ollitrault, *Phys. Rev.* **C82**, 034913 (2010), arXiv:1007.5469 [nucl-th].
- [13] H. Petersen, G.-Y. Qin, S. A. Bass, and B. Muller, *Phys. Rev.* **C82**, 041901 (2010), arXiv:1008.0625 [nucl-th].
- [14] R. A. Lacey, R. Wei, N. N. Ajitanand, and A. Taranenko, *Phys. Rev.* **C83**, 044902 (2011), arXiv:1009.5230 [nucl-ex].
- [15] D. Teaney and L. Yan, *Phys. Rev.* **C83**, 064904 (2011), arXiv:1010.1876 [nucl-th].
- [16] Z. Qiu and U. W. Heinz, *Phys. Rev.* **C84**, 024911 (2011), arXiv:1104.0650 [nucl-th].
- [17] J. Fu, *Phys. Rev.* **C92**, 024904 (2015).
- [18] H. Niemi, K. J. Eskola, and R. Paatelainen, *Phys. Rev.* **C93**, 024907 (2016), arXiv:1505.02677 [hep-ph].
- [19] J. Noronha-Hostler, L. Yan, F. G. Gardim, and J.-Y. Ollitrault, *Phys. Rev.* **C93**, 014909 (2016), arXiv:1511.03896 [nucl-th].
- [20] G. Aad et al. (ATLAS), *Phys. Rev.* **C92**, 034903 (2015), arXiv:1504.01289 [hep-ex].
- [21] J. Adam et al. (ALICE), *Phys. Rev. Lett.* **117**, 182301 (2016), arXiv:1604.07663 [nucl-ex].
- [22] R. A. Lacey, D. Reynolds, A. Taranenko, N. N. Ajitanand, J. M. Alexander, F.-H. Liu, Y. Gu, and A. Mwai, *J. Phys.* **G43**, 10LT01 (2016), arXiv:1311.1728 [nucl-ex].
- [23] T. Hirano, U. W. Heinz, D. Kharzeev, R. Lacey, and Y. Nara, *Phys.Lett.* **B636**, 299 (2006), arXiv:nucl-th/0511046 [nucl-th].
- [24] B. Schenke, S. Jeon, and C. Gale, *Phys.Rev.Lett.* **106**, 042301 (2011), arXiv:1009.3244 [hep-ph].
- [25] P. Bozek, M. Chojnacki, W. Florkowski, and B. Tomasik, *Phys.Lett.* **B694**, 238 (2010), arXiv:1007.2294 [nucl-th].
- [26] H. Niemi, G. Denicol, P. Huovinen, E. Molnar, and D. Rischke, *Phys.Rev.* **C86**, 014909 (2012), arXiv:1203.2452 [nucl-th].
- [27] P. Kovtun, D. Son, and A. Starinets, *Phys.Rev.Lett.* **94**, 111601 (2005), arXiv:hep-th/0405231 [hep-th].
- [28] R. S. Bhalerao, J.-Y. Ollitrault, and S. Pal, *Phys. Lett.* **B742**, 94 (2015), arXiv:1411.5160 [nucl-th].
- [29] L. Yan and J.-Y. Ollitrault, *Phys. Lett.* **B744**, 82 (2015), arXiv:1502.02502 [nucl-th].
- [30] R. S. Bhalerao, J.-Y. Ollitrault, and S. Pal, *Phys. Rev.* **C88**, 024909 (2013), arXiv:1307.0980 [nucl-th].
- [31] R. A. Lacey, A. Taranenko, N. Ajitanand, and J. Alexander, (2011), arXiv:1105.3782 [nucl-ex].
- [32] R. A. Lacey, Y. Gu, X. Gong, D. Reynolds, N. Ajitanand, et al., (2013), arXiv:1301.0165 [nucl-ex].
- [33] E. Shuryak and I. Zahed, (2013), arXiv:1301.4470 [hep-ph].
- [34] R. A. Lacey, P. Liu, N. Magdy, M. Csand, B. Schweid, N. N. Ajitanand, J. Alexander, and R. Pak, (2016), arXiv:1601.06001 [nucl-ex].
- [35] S. Acharya et al. (ALICE), *Phys. Lett.* **B773**, 68 (2017), arXiv:1705.04377 [nucl-ex].
- [36] K. Aamodt et al. (ALICE Collaboration), *Phys.Rev.Lett.* **107**, 032301 (2011), arXiv:1105.3865 [nucl-ex].
- [37] Pifeng Liu and Roy A. Lacey, to be published.
- [38] M. L. Miller, K. Reygers, S. J. Sanders, and P. Steinberg, *Ann. Rev. Nucl. Part. Sci.* **57**, 205 (2007); B. Alver et al., *Phys. Rev. Lett.* **98**, 242302 (2007).
- [39] K. Aamodt et al. (ALICE), *Phys. Rev. Lett.* **106**, 032301 (2011), arXiv:1012.1657 [nucl-ex].
- [40] G. Aad et al. (ATLAS), *Phys. Lett.* **B710**, 363 (2012), arXiv:1108.6027 [hep-ex].
- [41] D. A. Teaney, in *Quark-gluon plasma 4*, edited by R. C. Hwa and X.-N. Wang (2010) pp. 207–266, arXiv:0905.2433 [nucl-th].